Quaternary Science Reviews 284 (2022) 107506

Contents lists available at ScienceDirect

Quaternary Science Reviews

journal homepage: www.elsevier.com/locate/quascirev

Glacial-interglacial evolution of seasonal cooling events documented by land-snail eggs from Chinese loess

Fengjiang Li [a, b, c, *], Naiqin Wu [a, b, d, **], Dan Zhang [a, d], Denis-Didier Rousseau [e, f, g], Yiquan Yang [a, h], Qingzhen Hao [a, b, c, d], Yajie Dong [a, b, c], Houyuan Lu [a, d, i]

[a] Key Laboratory of Cenozoic Geology and Environment, Institute of Geology and Geophysics, Chinese Academy of Sciences, Beijing, 100029, China
[b] Innovation Academy for Earth Science, Chinese Academy of Sciences, Beijing, 100029, China
[c] CAS Center for Excellence in Life and Paleoenvironment, Beijing, 100044, China
[d] College of Earth and Planetary Sciences, University of Chinese Academy of Sciences, Beijing, 100049, China
[e] Geosciences Montpellier, University of Montpellier, 34095, Montpellier, France
[f] Institute of Physics-CSE, Division of Geochronology and Environmental Isotopes, Silesian University of Technology, Gliwice, Poland
[g] Lamont-Doherty Earth Observatory, Columbia University, Palisades, NY, 10964, USA
[h] Gansu Civil Air Defence, Lanzhou, 730010, China
[i] CAS Center for Excellence in Tibetan Plateau Earth Sciences, Beijing, 100101, China

ARTICLE INFO

Article history:
Received 29 November 2021
Received in revised form
2 April 2022
Accepted 2 April 2022
Available online xxx

Handling Editor: Giovanni Zanchetta

Keywords:
Seasonal cooling event
Glacial-interglacial cycle
Terrestrial mollusc egg
Loess
Paleoclimate
East Asia

ABSTRACT

The alternations of glacial and interglacial cycles are a classical feature of Quaternary climatic evolution and have been demonstrated to be closely related to seasonal insolation changes at high northern latitudes. Therefore, seasonal features may provide insights into glacial-interglacial cycles. However, mainly due to the lack of long time series of seasonally sensitive proxies, little is known about seasonal changes on the glacial-interglacial scale. The unhatched eggs preserved in sediments can serve as a proxy of seasonal cooling events (e.g., cold spells) since biological principles indicate that egg hatching is sensitive to temperature changes, and cooling-event-induced low temperatures during the reproductive season are unfavorable for eggs to hatch. Vertebrate eggs are well documented in the geological records, but they rarely provide continuous records through time. Here we present a high-resolution time series of land-snail eggs from the Chinese Loess Plateau, spanning the last three glacial-interglacial cycles. The results show that seasonal cooling events, indicated by peaks in egg abundance, are strong during glacial inceptions and climate cooling shifts of the marine isotope stages (MIS) 7e/7d, MIS 5e/5d, MIS 5c/5b and MIS 3/2. They tend not to occur during deglacials. They may result in low temperatures unfavorable for egg hatching during the reproductive season. Although several factors may be involved, seasonal cooling events in the Chinese Loess Plateau seem to be positively and more closely related to high-northern-latitude ice sheet growth. This finding may provide a new perspective for understanding glacial-interglacial evolution.

1. Introduction

Seasonal cooling events are well documented aspects of Earth's climate system and may have severe damage to ecosystems at longer timescales. However, although their occurrence is well documented by modern observations, less is known about their evolution at long timescales (e.g., Francis et al., 2009; Honda et al., 2009; Ivany et al., 2000; Petoukhov and Semenov, 2010; Wu et al., 2011; Vihma, 2014). Promisingly, several studies have implied that frequent seasonal cooling events on geological timescales may have caused severe damage to ecosystems or even led to the extinction or migration of organisms. A readjustment of dinosaur populations of the Late Triassic has been linked to cooler conditions (Kent and Clemmensen, 2021). A rapid 4 °C decrease in winter temperature, rather than annual temperature, is also likely to have caused the

* Corresponding author. Key Laboratory of Cenozoic Geology and Environment, Institute of Geology and Geophysics, Chinese Academy of Sciences, Beijing, 100029, China.
** Corresponding author. Key Laboratory of Cenozoic Geology and Environment, Institute of Geology and Geophysics, Chinese Academy of Sciences, Beijing, 100029, China.
E-mail addresses: fengjiangli@mail.iggcas.ac.cn (F. Li), nqwu@mail.iggcas.ac.cn (N. Wu).

https://doi.org/10.1016/j.quascirev.2022.107506
0277-3791/

mass extinctions among the marine fauna at the Eocene/Oligocene boundary when the East Antarctic ice sheet was substantially enlarged and the atmospheric CO_2 concentration was particularly lower (Ivany et al., 2000). However, long-term high-resolution records of seasonal cooling events are scarce, which strongly limits our understanding of how seasonal events evolved at timescales beyond that of modern observations.

Glacial-interglacial alternations, characterized by the growth and decay of ice sheets at high northern latitudes, are a fundamental aspect of Quaternary climatic evolution (e.g., Kukla et al., 1990; Lisiecki and Raymo, 2005; Rousseau et al., 2009; Hao et al., 2012). Seasonal changes, including seasonal events (e.g., cold spells), are likely to be a major causal factor of the associated climate dynamics (e.g., Milankovitch, 1941; Hays et al., 1976; Yin and Berger, 2010). Therefore, Quaternary glacial-interglacial alternations are potentially among the best scenarios documenting long-term high-resolution history of seasonal changes. However, research on climate change on glacial-interglacial timescales has long focused on astronomical and, more recently, millennial variabilities (Heinrich, 1988; Bond et al., 1992; Dansgaard et al., 1993; Barker et al., 2011; Rousseau et al., 2020). Although being a critical climate parameter (e.g., Ruddiman, 2001; Yin and Berger, 2010; Sima et al., 2009, 2013), seasonal changes have rarely been investigated on the glacial-interglacial timescale. Indeed, the lack of proxies sensitive to seasonal changes and associated long time series strongly limits such investigations (Petoukhov and Semenov, 2010; Gao et al., 2015).

Although plants are a reliable indicator of variations in seasonality (e.g., Zhang et al., 2020), fauna can be more valuable indicators. Among the various stages in the life cycle of animals, egg hatching is very sensitive to temperature changes during the reproductive season (Baur and Baur, 1993; Heller, 2001; Chen, 2006; Panigrahi, 2008; Myzyk, 2011). Eggs, therefore, have the potential to be a new and reliable proxy of seasonal cooling events (Li et al., 2021). However, our knowledge of fossil eggs comes mainly from dinosaurs and birds and these vertebrate eggs have rarely been used to study the evolution of seasonal events because they commonly have, like bone remains, a relatively discontinuous stratigraphic distribution (e.g., Miller et al., 1992; Wang et al., 2017). Fortunately, abundant land-snail eggs have recently been observed to distribute continuously, at least over the last 1.3 Ma, in the loess-paleosol sequences of the Chinese Loess Plateau (CLP), East Asia (Li et al., 2019). Moreover, samplings in modern environments across the continental climate gradient from the CLP to East China reveal that unhatched land-snail eggs are likely to be a proxy of cold spring events (Li et al., 2021).

The loess-paleosol sequences in the CLP have proven to be one of the most complete and sensitive terrestrial records of past environmental changes (e.g., Liu, 1985; Kukla and An, 1989; Guo et al., 2000). The alternations of loess and paleosol units record glacial-interglacial cycles which have been correlated with those revealed by the marine oxygen isotope record (e.g., Liu, 1985; Kukla et al., 1990; Hao et al., 2012). The paleosol (S) and loess (L) units over the last 350 kyr are classically labeled S3, L3, S2, L2, S1, L1 and S0, with very low values of magnetic susceptibility (MS) typical of loess units and higher values of paleosols (Fig. S1). The correlation of MS variations of loess-paleosol alternations with the marine isotope stages (MIS) of the global $\delta^{18}O$ stacked record (Lisiecki and Raymo, 2005) has been widely applied to establish timescales for Chinese loess deposits (e.g., Kukla et al., 1988, 1990; Ding et al., 1995; Wu et al., 2007; Rousseau et al., 2009; Hao et al., 2012). In the western CLP, loess deposits are characterized by thick loess units and thin, weakly-developed paleosol units (Liu, 1985).

In this study, we investigate the evolution of seasonal cooling events on the glacial-interglacial timescale with an average resolution of about 600–1000 yr. First, we present a high-resolution time series of land-snail eggs and shells from the Huining section spanning the last three glacial-interglacial cycles. Second, based on our recent studies (Li et al., 2021), we further confirm seasonal cooling events as the main potential factor controlling egg abundance. Third, we describe the changes in egg abundance and the evolution of seasonal cooling events during different stages of glacial-interglacial cycles for the last 350 kyr. Finally, we compare our results with other independent climatic/environmental indicators, enabling us to propose possible causes for the changes in seasonal cooling events.

Our results show that six seasonal cooling events only occur during climate cooling transitions, i.e. during interglacial-glacial transitions for the strongest ones and during warm-to-cold substage transitions, or interstadial-stadial transitions, for the others. They never occur during deglacials. These findings contribute to an improved understanding of the evolution of seasonal events on the glacial-interglacial scale, and may provide a new perspective for the characterisation of glacial-interglacial evolution.

2. Materials and methods

The Huining loess-paleosol sequence (36°14′N, 105°09′E, 2100 m above sea level) is located in the western CLP (Fig. 1A). The CLP, located in the East Asian monsoon region, has remained under the influence of ice volume changes in high northern latitudes since at least 2.6 Ma, mainly via the East Asian winter monsoon (Qian, 1991; Ding et al., 1995; Hao et al., 2012). The present climate over the CLP is characterized by seasonal alternations of the East Asian winter and summer monsoon circulations (Fig. 1A). In winter, the East Asian winter monsoon winds prevail, resulting in dry, cold climate conditions. In summer, the East Asian summer monsoon carries warm, moist air masses towards the CLP, causing heavy rainfall and warm climate conditions. The present climate over the CLP is also characterized by relatively frequent seasonal cooling events represented by cold spells. Some 40–70% of the annual total of cold spells occur in spring (mainly in April and May) (Qian, 1991; Han et al., 2013). They generate rapid temperature decreases of more than 8–10 °C within 3–7 days or more (Qian, 1991), causing low spring temperatures (Fig. 1B) and therefore a large numbers of snail eggs not to hatch (Li et al., 2021). The spring daily average temperature minima and maxima in the Huining region vary between 0.6–10.3 °C and 10.4–23.7 °C, respectively (http://data.cma.cn).

The field and laboratory work that was performed during 2017 and 2018 involved a slow and painstaking, but unavoidable, procedure. Because weathered sediments are meters thick on the outcrop of the Huining loess-paleosol sequence, we dug numerous deep columns to remove the thick weathered sediments and therefore correctly identify the loess and paleosol lithology (Fig. 2A); and then we extracted a continuous sequence of 526 sediment samples at a 10-cm interval from the top of L4 to S0 (Fig. 2B), using stratigraphic markers or horizontal lines to connect the successive steps of the section. Each sample corresponded to ~15 L, weighing about 15 kg (Fig. 2C). All samples corresponding to a total weight of ~8 t were manually carried from the gully to the ground (Fig. 2D). To reduce transportation costs of such a large amount of material, we used a mesh of 0.5-mm diameter to wash and sieve all the samples in the field (Fig. 2E and F) and then transported all the sieved samples to the laboratory for final sieving to concentrate the fossil material. Both eggs and shells were sorted under a stereomicroscope. We use international protocols of the Quaternary land snail studies (e.g., Wu et al., 2007; Rousseau et al., 2009) to identify and count complete shells and useful fragments enabling us to estimate the numbers of individuals for each species.

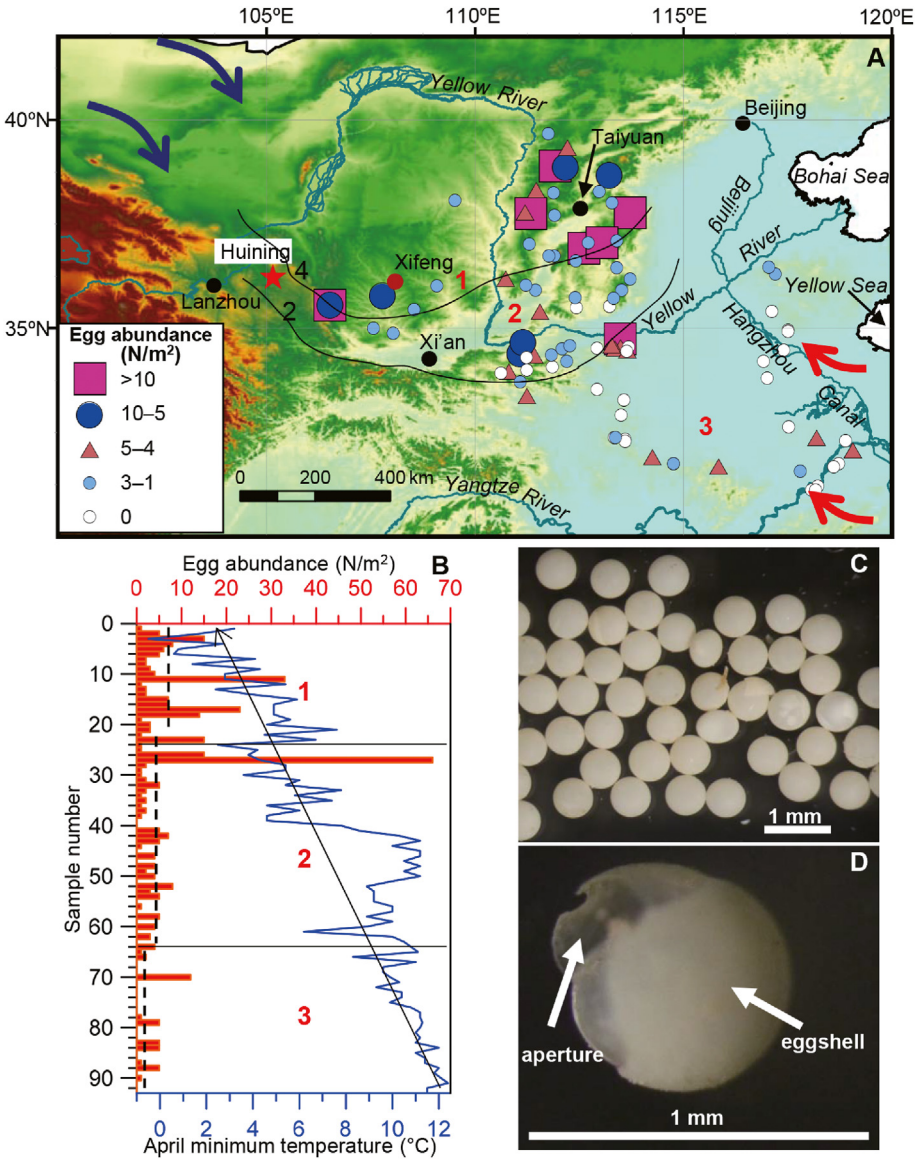

Fig. 1. (A) Map showing the location of the Huining section, surface-soil snail egg abundances (modified from Li et al., 2021) and the annual average frequency of cold spells (Qian, 1991). Red star: location of the Huining section. Red solid circle: location of the Xifeng section (mentioned in the text). Black solid circles: locations of major cities. Blue and red arrows: directions of the East Asian winter and summer monsoons, respectively. Black lines: annual average frequency of cold spells. Red numbers: zones of surface-soil egg abundance. (B) Variations in egg abundance and spring minimum temperature (modified from Li et al. (2021)). The temperature data are from the China Meteorological Data Service Center (http://data.cma.cn). Vertical dashed lines: the average of egg abundance in each zone. (C) Fossil snail eggs from the Huining section. (D) An embryonic shell partly visible inside an egg from the Huining section. (For interpretation of the references to color in this figure legend, the reader is referred to the Web version of this article.)

Eggs have been counted in parallel. The largest dimension of the eggs was measured under a Leica S9i microscope with a digital micrometer.

Parallel with the snail-egg samples, a total of 526 powder samples were taken for MS measurement. After the powder samples were air-dried in the laboratory, low-field MS values were measured, using a Bartington MS2 MS meter, to establish the local stratigraphy, with loess units having very low MS values and paleosols higher values (Fig. S1).

The timescale of the Huining section was established using age controls from the boundary ages of each MIS established by Lisiecki and Raymo (2005). Dates were then interpolated between them using an MS age model (Kukla et al., 1988, 1990). The average time resolution of the 10-cm sampling interval is 0.58 kyr for loess layers and 0.98 kyr for paleosols. The use of the MS model was justified for the following three reasons. First, soil development is very weak in the Huining stratigraphy (Figs. 2 and 3); therefore the sequence is composed of very thick loess units characterized by extremely low MS values and very thin paleosol layers. This characteristic indicates that the Huining sequence has a very weak soil development. Second, the chronological uncertainties between the MS and linear models are mostly (~80%) < 1 kyr (average of 0.67 kyr) (Fig. S2; Supplementary data), hence suitable for our study. Third, the time series based on the MS model provided an independent and extensively used timescale for the loess-paleosol sequence (e.g., Kukla et al., 1990).

3. Results

3.1. Snail eggs in the Huining loess-paleosol sequence

The eggs are spherical or flat-spherical in shape and yellow-

Fig. 2. Field operations: sampling, transport, washing and sieving of loess samples to extract land snails and their eggs. A: One of the columns with weathered sediments being removed from the surface of the outcrop before lithological description and sampling. B: Sampling for land snails and eggs. C: Examples of the samples; each bagged sample weighed ~15 kg. D: Samples being carried upward from the gully to the ground surface. E and F: Sieving of sediment samples in the field enabling the removal of sediments with grain size smaller than 0.5 mm diameter and favoring the collection of land-snails and eggs from the mesh in the laboratory.

white in color, and the eggshells are thin and calcified (Fig. 1C); nearly all of the eggs were intact. Some eggs contained a protoconch, i.e. the embryonic shell of land snails (Fig. 1D), confirming our initial assumption that they were laid by land snails. The size of the eggs varies between 0.6 and 0.8 mm in their largest dimension (Fig. 1C and D). Eggs of these small dimensions are laid by minute snails with a shell size of ~2–3 mm (Table S1) (Heller, 2001; Welter-Schultes, 2012). The species identified from the Huining loess-paleosol sequence are dominated by *Pupilla aeoli*, *Pupilla muscorum*, *Vallonia tenera* and *Cathaica pulveratricula*. The first three species have shell sizes of ~2–3 mm. Since *Pupilla muscorum* is most likely ovoviviparous (e.g., Pokryszko, 2001), *Vallonia tenera* and *Pupilla aeoli* are likely to be among the potential producers of these eggs, if the latter is not ovoviviparous.

3.2. Changes in egg abundance over the last three glacial-interglacial cycles

Based on their amplitude and duration, combined with changing amplitude analysis, six stages of high egg abundance (EA), numbered EA-6 to EA-1 (Table 1), were identified from the last three glacial-interglacial cycles. During the two earliest climate cycles, S3–L3 and S2–L2, high egg abundance occurred mostly during the transitions from paleosol to loess units, characterized by decreasing MS values (Fig. 3). However, in the last climate cycle, S1–L1, the pattern is more complex. Three peaks of egg abundance EA-3, EA-2 and EA-1 occur during the transitions between substages of the last climate cycle, but not during the glacial inception between S1 and L1 (corresponding to the MIS 5a/4 transition). This may be due to the greater complexity of both stratigraphic records and climate cyclicity of the last climate cycle. The S1 paleosol formed during the last interglacial (sensu lato) and included five substages corresponding to MIS 5e–5a, whereas the L1 unit accumulated during the last glacial and included three substages, MIS 3 being significantly milder than MIS 4 and MIS 2 (Figs. 3 and 4) (Ding et al., 1995; Lisiecki and Raymo, 2005; Sun et al., 2006; Rousseau et al., 2009; Hao et al., 2012). All the six EA stages over the last three glacial-interglacial cycles do not occur during the transitions from loess to paleosol, corresponding to deglacials, and they are largely absent in pure loess and paleosol units. Using correlation with the marine isotope stratigraphy, they correspond to the following climatic transitions: MIS 9/8, MIS 7e/7d, MIS 7a/6, MIS

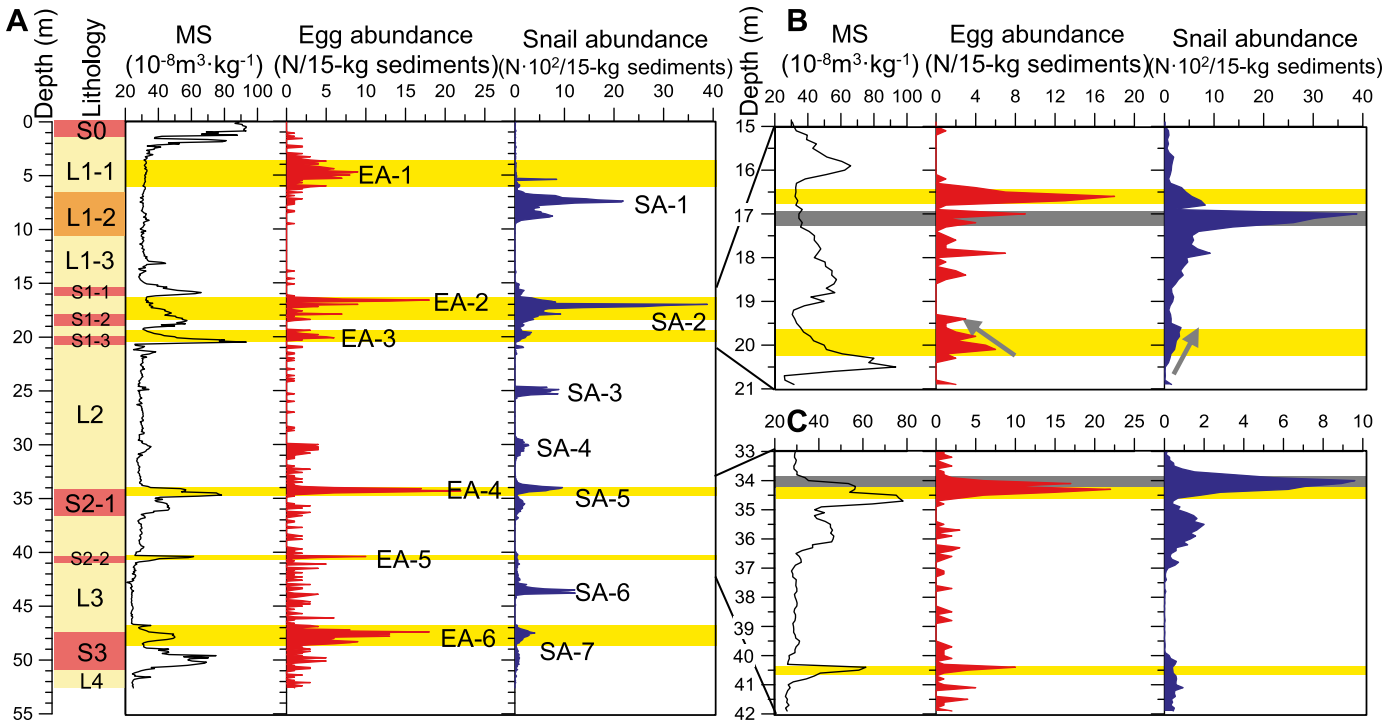

Fig. 3. Changes in magnetic susceptibility (MS) and egg and snail abundances over the last three climate cycles from the Huining section. A: Complete record together with the lithology. In the lithology column, the loess units (L1 to L4) are indicated by yellow shading and the paleosol units (S0 to S3) by red shading. The horizontal yellow bars correspond to stages of egg abundance (EA-1 to EA-6). The snail abundance (SA) stages are labeled SA-1 to SA-7. B: Enlargement of changes in egg and snail abundances from paleosol complexes S2 and S1. The grey bars indicate stages with low egg abundance and high snail abundance, underlining asynchronicity between both signals. The arrows indicate an interval with an inverse pattern of variation of egg and snail abundances. (For interpretation of the references to color in this figure legend, the reader is referred to the Web version of this article.)

Table 1
Depth, age, duration and abundance of each egg abundance (EA) stage in the Huining section.

EA stage	Depth (m)	Age (ka)	Duration (ka)	Total EAs (count in 15 kg of sediment)
EA-1	3.6–6.1	20.4–27.6	7.2	103
EA-2	16.4–18.4	86.1–95.4	9.3	76
EA-3	19.4–20.1	110.5–117.7	7.2	24
EA-4	34.0–34.6	190.2–198.6	8.4	78
EA-5	40.4–40.5	239.5–240.7	1.2	14
EA-6	46.8–48.6	295.9–313.2	17.3	129

5e/5d, MIS 5c/5b, and MIS 3/2 (Fig. 4). This indicates that high egg abundance occurred mainly during intervals of ice sheet growth, i.e., glacial inceptions, and during climate cooling shifts such as MIS 7e/7d, MIS 5e/5d and MIS 5c/5b.

Two groups of stages can be identified. The first group, G1, comprises EA-6 and EA-4, which occur around the boundary between an interglacial and a glacial, showing a high abundance during a relatively long time interval (Table 1, Fig. 4). The second group, G2, comprises EA-5, EA-3, EA-2 and EA-1, and occurs during climate cooling shifts of MIS 7e/7d, MIS 5e/5d, MIS 5c/5b and MIS 3/2. Among G2, EA-1 has a relatively high total abundance, corresponding to the unusual transition from the mild interval MIS 3 to the severe glacial maximum of MIS 2. The highest abundances in G2 are generally no greater than half of those in G1, although their duration is not significantly shorter than that of G1, except for EA-5 which lasted only 1.2 kyr (Fig. 4, Table 1).

Parallel to the egg occurrence, the snail abundance (SA) shows seven stages of high abundance, indicating seven periods potentially suitable for egg hatching and population increase, labeled SA-1 to SA-7, from top to bottom (Fig. 3). The highest snail abundance, during S1–L1 (the last climate cycle), is ~1–2 times higher than during the preceding S3–L3 and S2–L2 climate cycles. The most striking observation is that high snail abundance corresponds to low egg abundance (e.g., SA-1, SA-2, SA-3, SA-5 and SA-6); conversely, high egg abundance is mostly coupled with low snail abundance (e.g., EA-1, EA-2, EA-3, EA-4 and EA-6) (Fig. 3). Interestingly, the phase of anti-correlation between egg and snail abundance peaks seems to be different during glacials and interglacials. We propose that this may imply differences in seasonality during glacials and interglacials. Glacials and interglacials in the CLP have different dominant ecological groups of land snails (e.g., Li et al., 2006; Wu et al., 2018), and different ecological groups may have respective dominant seasons for their reproduction and growth (Wu et al., 2002; Huang et al., 2012; Dong et al., 2021). Therefore, it is possible that changes in the phase of anti-correlation during glacials and interglacials would be linked with the differences in the seasonalities favorable for the growth of different snail groups. Detailed studies are needed to seek the causes of this interesting phenomenon.

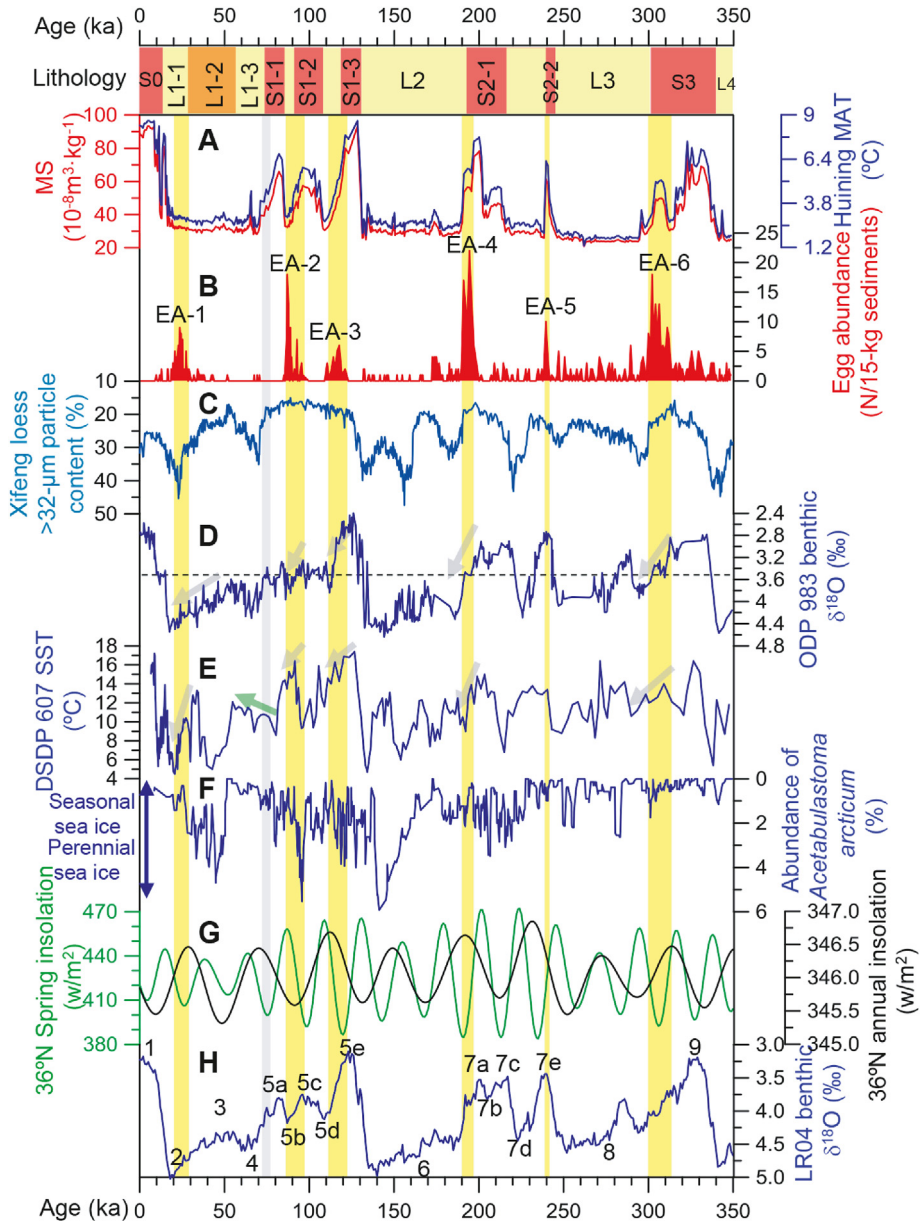

Fig. 4. Variations of egg abundance in the Huining section over the past 350 kyr and a comparison with other climate proxies. The lithology is characterized by alternations of loess (L1 to L4) and paleosol (S0 to S3) units. A: Magnetic susceptibility (MS) (red) and mean annual temperature (MAT) (blue) from the Huining section. The MAT was reconstructed using the model of Han et al. (1996). B: Record of land-snail egg abundance from the Huining section, with egg abundance stages labeled EA-1, EA-2 … EA-6. C: Record of the coarse grain-size component of the Xifeng section in the Chinese Loess Plateau (Hao et al., 2012). D: Benthic $\delta^{18}O$ record from Ocean Drilling Program (ODP) Site 983 (Raymo et al., 2004). The dashed line indicates the benthic $\delta^{18}O$ value of 3.5 per mil as a critical threshold of changes in ice sheets (McManus et al., 1999). E: Sea surface temperature (SST) record from Deep Sea Drilling Project (DSDP) Site 607 (Ruddiman et al., 1989). Grey arrows in D and E indicate phases of ice-sheet growth and SST decrease, respectively, and the green arrow a SST increase. F: Relative abundance of the sea-ice-related ostracod species *Acetabulastoma arcticum* in the Arctic Ocean (Cronin et al., 2019). G: Spring (green) and annual (black) insolation at 36°N, the latitude of the Huining section (Laskar et al., 2004). H: LR04 benthic $\delta^{18}O$ stack (Lisiecki and Raymo, 2005). Numbers indicate marine oxygen isotope stages (MIS), and sub-stages, with even and odd numbers corresponding to glacial and interglacial stages, respectively. (For interpretation of the references to color in this figure legend, the reader is referred to the Web version of this article.)

4. Discussion

4.1. Seasonal cooling events as the main factor impacting egg abundance

Embryonic snail shells were observed within some eggs (Fig. 1D), clearly indicating that the eggs we are studying are from snails. The intactness of nearly all eggshells indicates that they were well preserved and failed to hatch. Factors potentially impacting egg abundance are varied, including preservation, biological factors, and climatic conditions.

Carbonate dissolution is the most important factor influencing the preservation of shells and eggs in loess deposits. It occurs mainly in paleosols and is indicated by the highest MS values (e.g., Kukla and An, 1989; Wu et al., 2007; Rousseau et al., 2009; Hao et al., 2012). However, throughout the last three climatic cycles of the Huining section, MS values are very low, varying between 33 and 25 $\times$ $10^{-8}m^3kg^{-1}$ in loess units and between 83 and

$37 \times 10^{-8} m^3 kg^{-1}$ in paleosols (Figs. 3 and 4A). The paleosol layers are very thin (their most intensively pedogenized horizon is always less than 1 m thick); prominent carbonate nodules and other characteristics of soil development, such as clay coatings, are absent (Fig. 2A, B and F). Snail shells and eggs do not show clear evidence of dissolution or reprecipitation (Fig. 1C and D). These features are consistent with very low mean annual temperatures reconstructed for the last three glacial-interglacial cycles (Fig. 4A). In fact, applying the relationship linking surface-soil MS values over the entire China with temperature data, as proposed by Han et al. (1996), the last three glacials and interglacials at Huining experienced very low mean annual temperatures, varying between ~1.9 and 3.1 °C and ~3.5–7.9 °C, respectively. These temperature ranges are unfavorable for strong dissolution of carbonate. More importantly, asynchronous variations in the shell and egg abundances cannot be caused by carbonate dissolution (Fig. 3). Moreover, given that the shells are generally more abundant in paleosols and weak paleosols (L1-2) (Fig. 3), we can assume that changes in egg and snail abundance caused by dissolution are negligible. These lines of evidence indicate that preservation did not strongly influence egg abundance in the Huining region.

Biological factors seem unlikely to be responsible for the changes in egg abundance. Asynchronous variations in shell and egg abundances (Fig. 3) exclude changes in snail abundance as the main cause of changes in egg abundance. Nearly all eggs are intact, excluding any significative influence of predator consumption of the nutrients in the eggs (Barker, 2001). Egg cannibalism within a clutch is also unlikely since most minute snails lay single eggs and thus are not within a clutch (Heller, 2001; Welter-Schultes, 2012).

Abrupt cooling events during the reproductive season (spring in the CLP) can impact the egg abundance, and are therefore the most likely factor responsible for our observations (Li et al., 2021). Biological studies indicate that, although moisture has an impact, temperature is the most important limiting factor influencing egg hatching of all oviparous animals including land snails (e.g., Barker, 1985; Baur and Baur, 1993; Kozlowski, 2000; Chen, 2006; Panigrahi, 2008; Myzyk, 2011; Welter-Schultes, 2012). The present-day hatching temperatures of the observed minute snails are mostly concentrated within the range of 15–25 °C (occasionally with the lowest value of 10 °C) (Table S1), as summarized by Li et al. (2021) and references therein. When these thresholds are exceeded, the large majority of eggs fail to hatch (Baur and Baur, 1993; Myzyk, 2011; Welter-Schultes, 2012; Li et al., 2021). The dominant species in natural environment of the CLP are minute snails (e.g., Dong et al., 2019, 2020; Li et al., 2021), which reproduce mainly in spring (Chen, 2006; Cameron, 2016; Li et al., 2021). Coincidently, seasonal cooling events such as cold spells occur frequently in spring over the CLP (Qian, 1991; Han et al., 2013).

Our recent investigation of land-snail eggs in modern surface soils in China, although preliminary, further supports from a spatial coverage that seasonal cooling events are the main factor impacting changes in egg abundance (Li et al., 2021). The investigation reveals that changes in egg abundance are well correlated with the intensity and frequency of seasonal cooling events, with higher egg abundance in the entire CLP (Zones 1 and 2 in Fig. 1A) corresponding to stronger cold spells and lower spring temperatures (Fig. 1A and B). In the northwestern CLP, all of the modern sampling sites yielded eggs, with an average egg abundance of 7 N/m^2. Seasonal cooling events occur often, with annual average frequencies >4 (Qian, 1991) (Fig. 1A). They result in very low temperatures, with spring minimum temperatures <10 °C, and with more than 80% < 5 °C (Fig. 1B), which constitutes very unsuitable conditions for egg hatching. It should emphasize that the most intense cold spells (annual average frequencies >6) occur in the locations to northern and southern Taiyuan (Qian, 1991) where egg abundance is highest (Fig. 1A). In the southeastern CLP, a total of ~80% of the modern sampling sites yielded eggs, but the egg abundance is lower, with averages reduced to ~50% of that in the northwestern CLP (Fig. 1A and B). In this region, cold spells generally occur at a moderate frequency, with annual average values between 4 and 2 (Qian, 1991). However, in East China, egg abundance is only ~10% of that in the northwestern CLP, and here, cold spells have the weakest influence, causing only ~20% of the spring minimum temperatures <10 °C (Fig. 1B), i.e. 80% of the spring minimum temperatures are suitable for egg hatching (Li et al., 2021). Moveover, the spring temperature maxima in the CLP and East China rarely exceed 25 °C (Fig. S3) (http://data.cma.cn), i.e. the upper threshold of the hatching temperature for the investigated minute snails (Table S1) (e.g., Baur and Baur, 1993; Myzyk, 2011; Welter-Schultes, 2012). Therefore, hatching failures caused by high temperatures are largely excluded.

4.2. Possible causes of changes in the seasonal cooling events

During the last 350 kyr, egg stages mainly occur during interglacial-to-glacial transitions (glacial inceptions) and cooling shifts of MIS 7e/7d, MIS 5e/5d, MIS 5c/5b and MIS 3/2 (Fig. 4B), with high egg abundance mostly corresponding to increases in the coarse particle content of Chinese loess (Fig. 4C) (Hao et al., 2012). These transitions are also characterized by increases in benthic foraminiferal $\delta^{18}O$ values at Ocean Drilling Program (ODP) Site 983 (Fig. 4D) (Raymo et al., 2004). This site is located in the Gardar Drift at 60.4°N, 23.64°W and would have recorded the growth and decay of ice sheets mainly in high northern latitudes. Associated with ice sheet growth phases are decreases in sea surface temperature, as documented by Deep Sea Drilling Project (DSDP) Site 607 at 40°N, 32.97°W (Fig. 4E) (Ruddiman et al., 1989). Atmospheric CO_2 concentration decreased during glacial inceptions and warm-to-cold substage transitions (Lüthi et al., 2008). Additionally, during most of the egg stages the Arctic Ocean could have experienced less extended and less perennial sea ice cover over the year (Fig. 4F) (Cronin et al., 2010, 2019; Stein et al., 2017).

Within the foregoing climatic framework, the most intense cooling stages EA-6 and EA-4, and the second most intense stage EA-1, correspond to intervals of a stronger East Asian winter paleomonsoon indicated by a coarser grain size of the loess deposits in the CLP (Fig. 4C) (Hao et al., 2012). They occur during periods of major ice sheet growth crossing the critical threshold of the benthic $\delta^{18}O$ value of 3.5 per mil at high northern latitudes (Fig. 4D) (Raymo et al., 2004). They also occur during periods of contracted sea ice cover (mainly in summer–autumn) in the Arctic Ocean, as indicated by the low abundance (<2.5%) of the sea-ice-related ostracod species *Acetabulastoma arcticum* (Fig. 4F) (Cronin et al., 2010, 2019; Stein et al., 2017). The weaker stages, EA-5, EA-3 and EA-2, correspond to a weaker East Asian winter paleomonsoon, as indicated by finer grain sizes in the CLP (Fig. 4C) (Hao et al., 2012). They also correspond to the growth of ice sheets from smaller initial sizes at high northern latitudes (Fig. 4D) (Raymo et al., 2004) and to increased sea ice cover (most likely perennial sea ice) in the Arctic Ocean, as indicated by high percentages of *Acetabulastoma arcticum*, with the maximum of 5.84% being twice as high as during the stages of EA-6, EA-4 and EA-1 (Cronin et al., 2010, 2019). The shortest stage, EA-5, is synchronous with the second smallest continental ice sheet volume of the last 350 kyr (Fig. 4D) (Raymo et al., 2004). The weakest stage, EA-3, occurred when Northern Hemisphere ice sheets grew from their smallest size, as indicated by the lowest $\delta^{18}O$ values during the MIS 5e interglacial (Fig. 4D) (Raymo et al., 2004). Similarly extended sea ice cover in the Arctic Ocean, with the maximum percentage of *Acetabulastoma arcticum* reaching 3.65%, is also observed during EA-3 (Fig. 4F) (Cronin et al.,

2010, 2019).

No egg peaks were recorded during the transition from MIS 5a to MIS 4. The benthic $\delta^{18}O$ record at high northern latitudes shows no major increase in continental ice volume (Fig. 4D), although models show that there was a significant growth of the Fennoscandian ice sheet (Batchelor et al., 2019). Sea surface temperature at high northern latitudes do not show a pattern contrary to that during other egg abundance stages (Fig. 4E) (Ruddiman et al., 1989). By contrast, the transition from MIS 5a to MIS 4 concided with the Toba volcanic erruption that strongly impacted the environmental conditions in East Asia (Rousseau and Kukla, 2000). Probably by perturbing the oceanic circulation, the Toba eruption may have caused a longer cooling period (Rampino and Self, 1992) that may be unfavorable for the snails to reproduce, causing the paucity of both snails and eggs (Fig. 3).

Ice sheet growth in high northern latitudes and larger sea ice retreat in summer and autumn in the Arctic Ocean could have contributed to the enhancement of seasonal cooling events acorss the CLP. The growth of Northern Hemisphere ice sheets would have strengthened the Siberian High and thus increased the frequency and intensity of seasonal cooling events, including cold spells over the CLP (Qian, 1991; Ding et al., 1995; Denton et al., 2005; Hao et al., 2012). Sea ice has strong impacts on climate instability through regulating the albedo of the sea surface and acting as a modulator of heat and moisture exchange between the ocean and the atmosphere (e.g., Wu et al., 2011; Vihma, 2014; Gao et al., 2015). Low sea ice cover would increase the exchange of heat and moisture between the ocean and the atmosphere and also decrease the albedo. This would favor strong air movements from high to middle northern latitudes including the CLP and therefore trigger strong cold spells. Atmospheric studies have demonstrated that summer–autumn sea ice loss intensified cold spells in the CLP during the following winter and spring (e.g., Francis et al., 2009; Honda et al., 2009; Petoukhov and Semenov, 2010; Wu et al., 2011; Vihma, 2014; Gao et al., 2015). Moreover, sea ice loss can also strengthen the Siberian High and thereby seasonal cooling events and cold spells in the CLP (Wu et al., 2011). During cold spells, the rapid temperature decreases of over 8–10 °C would have exceeded the lower threshold of 15–10 °C (Qian, 1991; Han et al., 2013), leading to substantial hatching failures.

Conversely, smaller Northern Hemisphere ice sheets associated with perennial (permanent) sea ice cover in the Arctic Ocean would have favored increased air mass stability at high northern latitudes (Qian, 1991; Ding et al., 1995; Denton et al., 2005; Wu et al., 2011; Hao et al., 2012). As a result, seasonal cooling events would have been weakened, promoting increased egg hatching success and therefore reducing the egg abundance in the CLP.

Finally, most egg stages appear to be linked more to low spring insolation than to minima in annual insolation at 36°N (Fig. 4G) (Laskar et al., 2004), supporting the role of seasonal variations as the potential major limiting factor of snail egg hatching. Low spring insolation is likely to be a background factor to favor temperature decreases and thereby contribute to cooler seasonal environmental conditions during these particular intervals. Insolation as a background factor can also be supported by the fact that spring insolation minima around 330, 280, 170 and 140 ka do not induce prominent seasonal cooling events. Moreover, when noting that most of the time intervals with relatively higher insolation minima (greater than 400 w/m^2) do not yield prominent cold spells, it is worth checking if there is a threshold of spring insolation minimum for the occurrence of seasonal cooling events.

5. Conclusion

We have produced the first long time series of land-snail egg abudance from the western CLP. Six seasonal cooling events, indicated by high egg abundance, occurred during times of northern ice sheet growth, i.e. glacial inceptions, and the cooling transitions of MIS 7e/7d, MIS 5e/5d, MIS 5c/5b and MIS 3/2. However, no egg-abundance peaks are documented during deglacials, full glacials and most interglacials, indicating that seasonal cooling events were not prominent during these periods. The seasonal cooling events correspond well to growth phases of ice sheets at high northern latitudes and limited sea ice cover in the Arctic Ocean. Both ice sheet growth at high northern latitudes and limited sea ice cover in the Arctic Ocean, associated with decreases in atmospheric CO_2 concentration, would likely have triggered strong seasonal cooling events (represented by cold spells) in the CLP. The cold spells, associated with low local spring insolation, would have resulted in low temperatures unsuitable for egg hatching.

Our findings highlight the value of fossil land-snail eggs as environmental indicators that can yield new insights into past climate changes. Our study provides the first evidence indicating that strong seasonal cooling events occurred in East Asia during climatic transitions characterized by ice sheet growth at high northern latitudes over the last 350 kyr. This contributes to an improved understanding of seasonality changes at the glacial-interglacial scale. Future research should extend the dataset to older glacial-interglacial cycles, enabling the investigation of the impact of seasonal cold spells over the entire Quaternary.

Data availability statement

The data obtained by this work can be found in the supporting information.

Credit author statement

F.L. and N.W. conceived and designed the study. D.Z., Y.Y., F.L., Q.H., Y.D. and N.W. performed the sampling, collecting and counting of snail eggs and individuals. D.Z. and Y.Y. performed the magnetic susceptibility measurements. D.Z. and Q.H. established the chronology of the studied section. F.L., N.W. and D.D.R. wrote the manuscript. F.L., N.W., H.L., Y.Y., D.D.R and Y.D. contributed to the interpretation of the results and all authors provided inputs to the manuscript.

Declaration of competing interest

The authors declare that they have no known competing financial interests or personal relationships that could have appeared to influence the work reported in this paper.

Acknowledgments

We thank Drs Daojing Wang, Yueting Zhang and Xinbo Gao for assistance in the field work. We are grateful to the reviewers and the editor for careful and insightful comments and suggestions that improved the manuscript greatly. This study was supported by the National Natural Science Foundation of China (41888101, 42172210, T2192950 and 41371212) and the Strategic Priority Research Program of Chinese Academy of Sciences (XDB26000000). This is a Lamont-Doherty Earth Observatory (LDEO) contribution.

Appendix A. Supplementary data

Supplementary data to this article can be found online at https://doi.org/10.1016/j.quascirev.2022.107506.

References

Barker, G.M., 1985. Aspects of the biology of *Vallonia excentrica* (Mollusca: Vallonidae) in waikato pastures. In: Chapman, R.B. (Ed.), Proceedings of the 4th Australasian Conference on Grassland Invertebrate Ecology: Idaho. Caxton Press, pp. 64–70.

Barker, G.M., 2001. The Biology of Terrestrial Molluscs. CABI Publishing, Hamilton, p. 558.

Barker, S., Knorr, G., Edwards, R.L., Parrenin, F., Putnam, A.E., Skinner, L.C., Wolff, E., Ziegler, M., 2011. 800,000 years of abrupt climate variability. Science 334, 347–351.

Batchelor, C.L., Margold, M., Krapp, M., Murton, D.K., Dalton, A.S., Gibbard, P.L., Stokes, C.R., Murton, J.B., Manica, A., 2019. The configuration of Northern Hemisphere ice sheets through the Quaternary. Nat. Commun. 10, 3713. https://doi.org/10.1038/s41467-019-11601-2.

Baur, B., Baur, A., 1993. Climatic warming due to thermal radiation from an urban area as possible cause for the local extinction of a land snail. J. Appl. Ecol. 30, 333–340.

Bond, G., Heinrich, H., Broecker, W., Labeyrie, L., McManus, J., Andrews, J., Huon, S., Jantschik, R., Clasen, S., Simet, C., Tedesco, K., Klas, M., Bonani, G., Ivy, S., 1992. Evidence for massive discharges of icebergs into the North Atlantic ocean during the last glacial period. Nature 360, 245–249.

Cameron, R., 2016. Slugs and Snails. William Collins, London, p. 508.

Chen, D.N., 2006. Culture Technology of Edible Land Snails. Jindun Press, Beijing, p. 110.

Cronin, T.M., Gemery, L., Briggs Jr., W.M., Jakobsson, M., Polyak, L., Brouwers, E.M., 2010. Quaternary Sea-ice history in the Arctic Ocean based on a new Ostracode sea-ice proxy. Quat. Sci. Rev. 29, 3415–3429.

Cronin, T.M., Keller, K.J., Farmer, J.R., Schaller, M.F., O'Regan, M., Poirier, R., Coxall, H., Dwyer, G.S., Bauch, H., Kindstedt, I.G., Jakobsson, M., Marzen, R., Santin, E., 2019. Interglacial paleoclimate in the arctic. Paleoceanogr. Paleoclimatol. 34, 1959–1979.

Dansgaard, W., Johnsen, S.J., Clausen, H.B., Dahl-Jensen, D., Gundestrup, N.S., Hammer, C.U., Hvidberg, C.S., Steffensen, J.P., Sveinbjörnsdottir, A.E., Jouzel, J., Bond, G., 1993. Evidence for general instability of past climate from a 250-kyr ice-core record. Nature 364, 218–220.

Denton, G.H., Alley, R.B., Comer, G.C., Broecker, W.S., 2005. The role of seasonality in abrupt climate change. Quat. Sci. Rev. 24, 1159–1182.

Ding, Z., Liu, T., Yu, Z., Guo, Z., Zhu, R., 1995. Ice-volume forcing of East Asian winter monsoon variations in the past 800,000 years. Quat. Res. 44, 149–159.

Dong, Y.J., Wu, N.Q., Li, F.J., Chen, X.Y., Zhang, D., Zhang, Y.T., Huang, L.P., Wu, B., Lu, H.Y., 2019. Influence of monsoonal water-energy dynamics on terrestrial mollusk species-diversity gradients in northern China. Sci. Total Environ. 676, 206–214.

Dong, Y.J., Wu, N.Q., Li, F.J., Zhang, D., Zhang, Y.T., Huang, L.P., Chen, X.Y., Wu, B., Lu, H.Y., 2020. Anthropogenic modification of soil communities in northern China for at least two millennia: evidence from a quantitative mollusk approach. Quat. Sci. Rev. 248, 106579.

Dong, Y.J., Wu, N.Q., Li, F.J., Huang, L.P., Lu, H.Y., Stenseth, N.C., 2021. Paleorecords reveal the increased temporal instability of species diversity under biodiversity loss. Quat. Sci. Rev. 269, 107147.

Francis, J.A., Chan, W., Leathers, D.J., Miller, J.R., Veron, D.E., 2009. Winter north hemisphere weather patterns remember summer Arctic sea-ice extent. Geophys. Res. Lett. 36, L07503. https://doi.org/10.1029/2009GL037274.

Gao, Y., Sun, J.Q., Li, F., He, S.P., Sandven, S., Yan, Q., Zhang, Z.S., Lohmann, K., Keenlyside, N., Furevik, T., Suo, L.L., 2015. Arctic sea ice and Eurasian climate: a review. Adv. Atmos. Sci. 32, 92–114.

Guo, Z.T., Biscaye, P., Wei, L.Y., Chen, X.H., Peng, S.Z., Liu, T.S., 2000. Summer monsoon variations over the last 1.2 Ma from the weathering of loess-soil sequences in China. Geophys. Res. Lett. 27, 1751–1754.

Han, H.H., Wang, Y.R., Huang, F., Wang, P., 2013. The characteristics of low temperature in spring over Loess Plateau. J. Gansu Sci. 25, 58–61.

Han, J.M., Lu, H.Y., Wu, N.Q., Guo, Z.T., 1996. The magnetic susceptibility of modern soils in China and its use for paleoclimate reconstruction. Studia Geophys. Geod. 40, 262–275.

Hao, Q.Z., Wang, L., Oldfield, F., Peng, S.Z., Qin, L., Song, Y., Xu, B., Qiao, Y.S., Bloemendal, J., Guo, Z.T., 2012. Delayed build-up of Arctic ice sheets during 400000-year minima in insolation variability. Nature 490, 393–396.

Hays, J.D., Imbrie, J., Shackleton, N.J., 1976. Variations in the Earth's orbit: pacemaker of the ice ages. Science 194, 1121–1132.

Heinrich, H., 1988. Origin and consequences of cyclic ice rafting in the northeast Atlantic Ocean during the past 130,000 years. Quat. Res. 29, 142–152.

Heller, J., 2001. Life history strategies. In: Barker, G.M. (Ed.), The Biology of Terrestrial Molluscs. CABI Publishing, Hamilton, pp. 413–445.

Honda, M., Inoue, J., Yamane, S., 2009. Influence of low Arctic sea-ice minima on anomalously cold Eurasian winters. Geophys. Res. Lett. 36, L08707. https://doi.org/10.1029/2008GL037079.

Huang, L.P., Wu, N.Q., Gu, Z.Y., Chen, X.Y., 2012. Variability of snail growing season at the Chinese Loess Plateau during the last 75 ka. Chin. Sci. Bull. 57, 1036–1045.

Ivany, L.C., Patterson, W.P., Lohmann, K.C., 2000. Cooler winters as a possible cause of mass extinctions at the Eocene/Oligocene boundary. Nature 407, 887–890.

Kent, D.V., Clemmensen, L.B., 2021. Northward dispersal of dinosaurs from Gondwana to Greenland at the mid-Norian (215–212 Ma, Late Triassic) dip in atmospheric pCO2. Proc. Natl. Acad. Sci. U.S.A. 118, e2020778118. https://doi.org/10.1073/pnas.2020778118.

Kozlowski, J., 2000. Reproduction of *Arion lusitanicus* Mabille, 1868 (Gastropoda: Pulmonata: Arionidae) introduced in Poland. Folia Malacol. 8, 87–94.

Kukla, G., An, Z.S., 1989. Loess stratigraphy in central China. Palaeogeogr. Palaeoclimatol. Palaeoecol. 72, 203–225.

Kukla, G., Heller, F., Liu, X.M., Xu, T.C., Liu, T.S., An, Z.S., 1988. Pleistocene climates in China dated by magnetic susceptibility. Geology 16, 811–814.

Kukla, G., An, Z.S., Melice, J.L., Gavin, J., Xiao, J.L., 1990. Magnetic susceptibility record of Chinese loess. Trans. R. Soc. Edinb. Earth Sci. 81, 263–288.

Laskar, J., Robutel, P., Joutel, F., Gastineau, M., Correia, A.C.M., Levrard, B., 2004. A long-term numerical solution for the insolation quantities of the Earth. Astron. Astrophys. 428, 261–285.

Li, F.J., Wu, N.Q., Pei, Y.P., Hao, Q.Z., Rousseau, D.D., 2006. Wind-blown origin of Dongwan late Miocene-Pliocene dust sequence documented by land snail record in western Chinese Loess Plateau. Geology 34, 405–408.

Li, F.J., Yang, Y.Q., Wu, N.Q., Huang, L.P., Dong, Y.J., 2019. Fossil snail eggs discovered from the Chinese Loess Plateau and their indications of seasonal abrupt climate event. Quat. Sci. 39, 1068–1070.

Li, F.J., Wu, N.Q., Dong, Y.J., Zhang, D., Zhang, Y.T., Yang, Y.Q., Huang, L.P., Xu, D.K., Zhang, J.P., Lu, H.Y., 2021. Land-snail eggs as a proxy of abrupt climatic cooling events during the reproductive season. Sci. Bull. 66, 1274–1277.

Lisiecki, L.E., Raymo, M.E., 2005. A Pliocene-Pleistocene stack of 57 globally distributed benthic δ18O records. Paleoceanography 20, PA1003. https://doi:10.1029/2004PA001071.

Liu, T., 1985. Loess and the Environment. China Ocean Press, Beijing, p. 251.

Lüthi, D., Le Floch, M., Stocker, T.F., Bereiter, B., Blunier, T., Barnola, J.M., Siegenthaler, U., Raynaud, D., Jouzel, J., 2008. High-resolution carbon dioxide concentration record 650,000-800,000 years before present. Nature 453, 379–382.

McManus, J.F., Oppo, D.W., Cullen, J.L., 1999. A 0.5-million-year record of millennial-scale climate variability in the North Atlantic. Science 283, 971–975.

Milankovitch, M., 1941. Kanon der Erdbestrahlung und seine Anwendung auf das Eiszeitenproblem: stamparija Mihaila Ćurčića; Canon of Insolation and the Ice-age Problem [English transl.]. Royal Serbian Academy of Sciences, Special Publication 132, Section of Mathematical and Natural Sciences 33, 1–633.

Miller, G.H., Beaumont, P.B., Jull, A.J.T., Johnson, B., 1992. Pleistocene geochronology and palaeothermometry from protein diagenesis in ostrich eggshells: implications for the evolution of modern humans. Philos. Trans. R. Soc. B Biol. Sci. 337, 149–157.

Myzyk, S., 2011. Contribution to the biology of ten Vertiginid species. Folia Malacol. 19, 55–80.

Panigrahi, A., 2008. Temperature effect on speed of development and rate of hatching of eggs of the giant pestiferous land snail *Achatina fulica* Bowdich. Indian Biol. 40, 23–26.

Petoukhov, V., Semenov, V.A., 2010. A link between reduced Barents-Kara sea ice and cold winter extremes over northern continents. J. Geophys. Res. 115, D21111. https://doi.org/10.1029/2009JD013568.

Pokryszko, 2001. Observations on seasonal dynamics of age structure and reproduction of *Pupilla muscorum* L. (Gastropoda: Pulmonata: Pupillidae). Folia Malacol. 9, 45–50.

Qian, L.Q., 1991. Climate of Loess Plateau. Meteorological Press, Beijing, p. 369.

Rampino, M.R., Self, S., 1992. Volcanic winter and accelerated glaciation following the Toba super-eruption. Nature 359, 50–52.

Raymo, M.E., Oppo, D.W., Flower, B.P., Hodell, D.A., McManus, J.F., Venz, K.A., Kleiven, K.F., McIntyre, K., 2004. Stability of North Atlantic water masses in face of pronounced climate variability during the Pleistocene. Paleoceanography 19, PA2008. https://doi:10.1029/2003PA000921.

Rousseau, D.D., Kukla, G., 2000. Abrupt retreat of summer monsoon at the S1/L1 boundary in China. Global Planet. Change 26, 189–198.

Rousseau, D.D., Wu, N.Q., Pei, Y.P., Li, F.J., 2009. Three exceptionally strong East-Asian summer monsoon events during glacial times in the past 470 kyr. Clim. Past 5, 157–169.

Rousseau, D.D., Antoine, P., Boers, N., Lagroix, F., Ghil, M., Lomax, J., Fuchs, M., Debret, M., Hatté, C., Moine, O., Gauthier, C., Jordanova, D., Jordanova, N., 2020. Dansgaard–Oeschger-like events of the penultimate climate cycle: the loess point of view. Clim. Past 16, 713–727.

Ruddiman, W.F., 2001. Earth's Climate: Past and Future. W.H. Freeman and Company, New York, p. 465.

Ruddiman, W.F., Raymo, M.E., Martinson, D.G., Clement, B.M., Backman, J., 1989. Pleistocene evolution: northern hemisphere ice sheet and north atlantic ocean. Paleoceanography 4, 353–412.

Sima, A., Rousseau, D.D., Kageyama, M., Ramstein, G., Schulz, M., Balkanski, Y., Antoine, P., Dulac, F., Hatté, C., 2009. Imprint of North-Atlantic abrupt climate changes on western European loess deposits as viewed in a dust emission model. Quat. Sci. Rev. 28, 2851–2866.

Sima, A., Kageyama, M., Rousseau, D.D., Ramstein, G., Balkanski, Y., Antoine, P., Hatté, C., 2013. Modeling dust emission response to North Atlantic millennial-scale climate variations from the perspective of East European MIS 3 loess deposits. Clim. Past 9, 1385–1402.

Stein, R., Fahl, K., Gierz, P., Niessen, F., Lohmann, G., 2017. Arctic Ocean sea ice cover during the penultimate glacial and the last interglacial. Nat. Commun. 8. https://doi.org/10.1038/s41467-017-00552-1.

Sun, Y.B., Chen, J., Clemens, S.C., Liu, Q.S., Ji, J.F., Tada, R., 2006. East Asian monsoon variability over the last seven glacial cycles recorded by a loess sequence from the northwestern Chinese Loess Plateau. Geochem. Geophy. Geosy. 7, Q12Q02. https://doi.org/10.1029/2006GC001287.

Vihma, T., 2014. Effects of Arctic Sea ice decline on weather and climate: a review. Surv. Geophys. 35, 1175–1214.

Wang, X.L., Kellner, A.W.A., Jiang, S.X., Cheng, X., Wang, Q., Ma, Y.X., Paidoula, Y., Rodrigues, T., Chen, H., Sayão, J.M., Li, N., Zhang, J.L., Bantim, R.A.M., Meng, X., Zhang, X.J., Qin, R., Zhou, Z.H., 2017. Egg accumulation with 3D embryos provides insight into the life history of a pterosaur. Science 358, 1197–1201.

Welter-Schultes, F., 2012. European Non-marine Molluscs, a Guide for Species Identification. Planet Poster Editions, Gottingen, p. 679.

Wu, B.Y., Su, J.Z., Zhang, R.H., 2011. Effects of autumn-winter Arctic sea ice on winter Siberian High. Chin. Sci. Bull. 56, 3220–3228.

Wu, N.Q., Liu, T.S., Liu, X.P., Gu, Z.Y., 2002. Mollusk record of millennial climate variability in the Loess Plateau during the last glacial maximum. Boreas 31, 20–27.

Wu, N.Q., Chen, X.Y., Rousseau, D.D., Li, F.J., Pei, Y.P., Wu, B., 2007. Climatic conditions recorded by terrestrial mollusc assemblages in the Chinese Loess Plateau during marine Oxygen Isotope Stages 12–10. Quat. Sci. Rev. 26, 1884–1896.

Wu, N.Q., Li, F.J., Rousseau, D.D., 2018. Terrestrial mollusk records from Chinese loess sequences and changes in the East Asian monsoonal environment. J. Asian Earth Sci. 155, 35–48.

Yin, Q.Z., Berger, A., 2010. Insolation and CO2 contribution to the interglacial climate before and after the Mid-Brunhes Event. Nat. Geosci. 3, 243–246.

Zhang, J.P., Lu, H.Y., Jia, J.W., Shen, C.M., Wang, S.Y., Chu, G.Q., Wang, L., Cui, A.N., Liu, J.Q., Wu, N.Q., Li, F.J., 2020. Seasonal drought events in tropical East Asia over the last 60,000 y. Proc. Natl. Acad. Sci. U.S.A. 117, 30988–30992.